catalysts

MDPI

Supporting Information

Hard Template-Assisted Trans-Crystallization Synthesis of Hierarchically Porous Cu-SSZ-13 with Enhanced NH_3-SCR Performance

Fuzhen Yang, Ying Xin *, Xiaoli Zhu, Ahui Tang, Long Yu, Dongxu Han, Junxiu Jia, Yaning Lu and Zhaoliang Zhang

Shandong Provincial Key Laboratory of Fluorine Chemistry and Chemical Materials, School of Chemistry and Chemical Engineering, University of Jinan, Jinan 250022, China; 17860733583@163.com (F.Y.); 18369838905@163.com (X.Z.); 202121100497@stu.ujn.edu.cn (A.T.); 202221201247@stu.ujn.edu.cn (L.Y.); 17824030075@163.com (D.H.); jjxcca@163.com (J.J.); sdlyn1999@163.com (Y.L.); chm_zhangzl@ujn.edu.cn (Z.Z.)

* Correspondence: chm_xiny@ujn.edu.cn; Tel.: +86-531-8973-6032

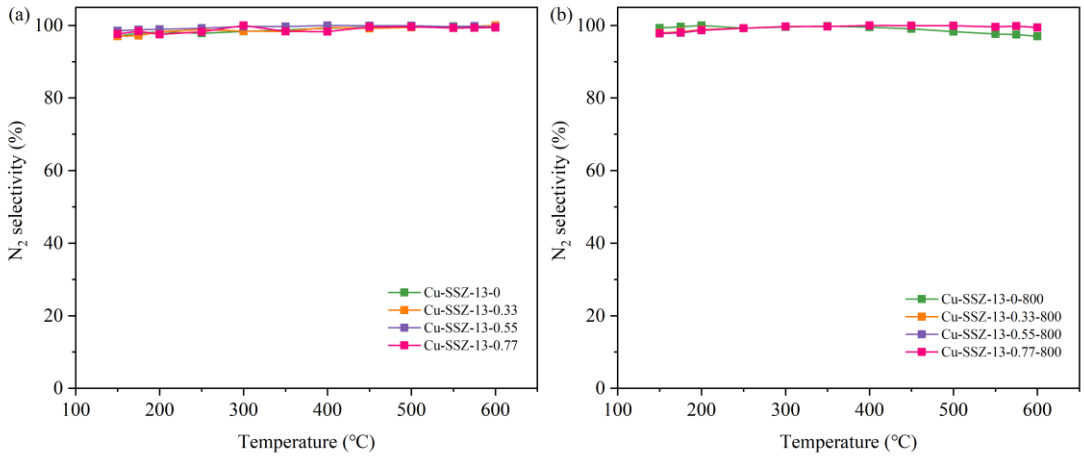

Figure S1. N_2 selectivity of (a) Cu-SSZ-13-*x* and (b) Cu-SSZ-13-*x*-800 catalysts.

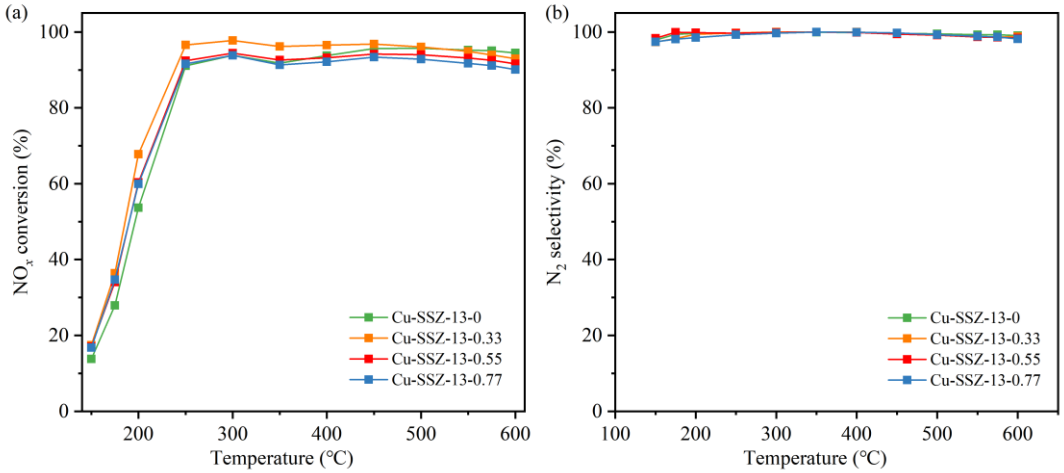

Figure S2. (a) NO_x conversion and (b) N_2 selectivity of Cu-SSZ-13-*x* catalysts at a gas hourly space velocity of 800,000 h^{-1}.

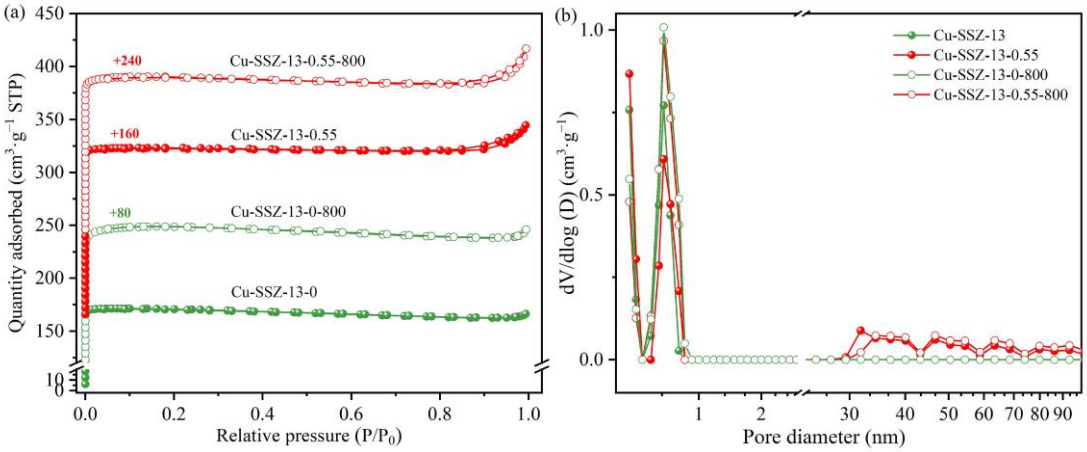

Figure S3. (a) N_2 adsorption/desorption isotherms and (b) pore size distribution curves of Cu-SSZ-13-0 and Cu-SSZ-13-0.55 catalysts before and after hydrothermal aging.

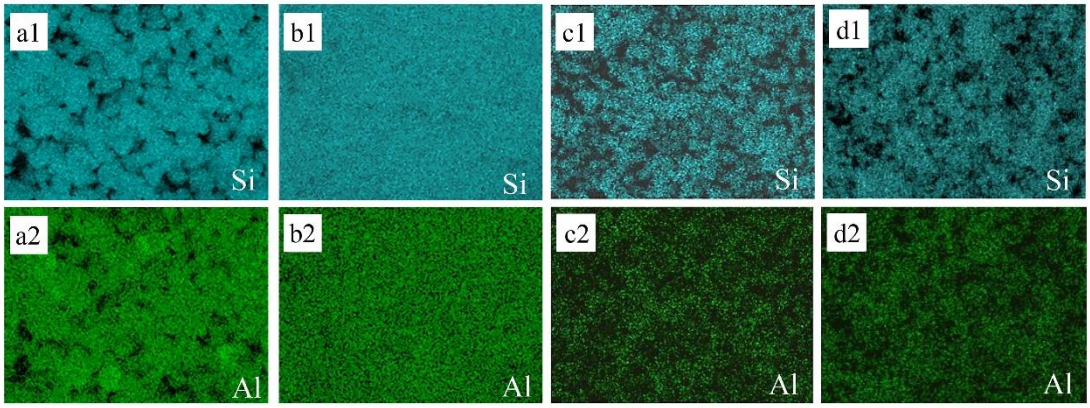

Figure S4. Si and Al elements EDS mappings of (a) Cu-SSZ-13-0, (b) Cu-SSZ-13-0.55, (c) Cu-SSZ-13-0-800, and (d) Cu-SSZ-13-0.55-800. (1) distribution of Si element and (2) distribution of Al element.

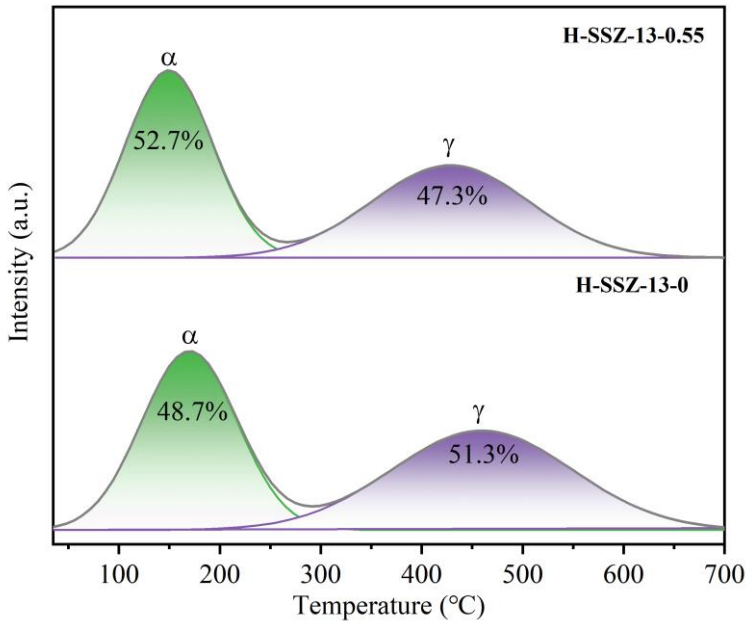

Figure S5. NH_3-TPD curves of H-SSZ-13-0 and H-SSZ-13-0.55 zeolites.

Table S1. Quantification of NH_3-TPD results for H-SSZ-13-0 and H-SSZ-13-0.55 zeolites.

Sample	NH_3 Desorption Amount (μmol·g^{-1})		
	Weak Acidity	Strong Acidity	Total Acidity
H-SSZ-13-0	703	740	1443
H-SSZ-13-0.55	931	835	1766

Table S2. Kinetic catalytic performances of Cu-SSZ-13-0 and Cu-SSZ-13-0.55 catalysts before and after hydrothermal aging.

Temperature (°C)	Cu-SSZ-13-0		Cu-SSZ-13-0.55		Cu-SSZ-13-0-800		Cu-SSZ-13-0.55-800	
	NO_x Conversion (%)	Reaction Rate×10^{-8} (mol·S^{-1}·g^{-1})	NO_x Conversion (%)	Reaction Rate×10^{-8} (mol·S^{-1}·g^{-1})	NO_x Conversion (%)	Reaction Rate×10^{-8} (mol·S^{-1}·g^{-1})	NO_x Conversion (%)	Reaction Rate×10^{-8} (mol·S^{-1}·g^{-1})
130	9.4	58.22	7.4	46.01	-	-	-	-
135	10.4	63.88	8.9	54.62	4.2	22.13	4.2	21.90
140	12.3	74.44	11.7	70.80	4.6	24.09	4.6	23.83
145	14.1	84.75	13.4	80.20	5.3	27.09	5.7	28.99
150	15.8	93.59	15.5	91.90	5.7	28.95	6.8	34.02
155	18.3	107.08	17.6	103.33	6.5	32.90	7.6	37.87
160	20.6	119.05	20.8	120.67	8.0	39.95	8.7	42.68
165	-	-	-	-	8.9	43.69	10.2	49.46
170	-	-	-	-	10.2	49.42	12.3	59.16
175	-	-	-	-	12.1	58.10	14.6	69.67
180	-	-	-	-	14.2	67.60	17.4	81.94